A Fast Kernel Is Not a Ship: Field Lessons from Agentic Optimization in vLLM

Jin Huang, Shuai Zhang, Jiading Gai, Vihang Patil,
Kailash Budhathoki, Ashish Khetan, Onkar Dabeer

Amazon Web Services
{jinhun, shuaizs, jiadingg, pvihang, kaibud, khetan, onkardab}@amazon.com

Abstract

Recent frontier language models are increasingly capable of technical work, yet measurable productivity gains from AI remain uneven. GPU optimization illustrates this gap: recent research shows that LLM agents can generate competitive GPU kernels, but typically only evaluates the kernel in isolation. Whether those kernels survive framework integration under production settings, preserve model behavior, and improve a system-level metric is rarely studied. We present AMMO (Agentic Model-on-Machine Optimizer), a *graph engineering* system built on top of a commodity agent harness that carries GPU optimizations across that last mile, from isolated win to deployment-measured change, for production vLLM deployments. Across four deployments on NVIDIA Hopper and Blackwell GPUs, AMMO autonomously discovered, implemented, and validated the changes behind four public vLLM pull requests (open or draft; none yet merged): measured end-to-end latency reductions range from 1.7% to 35.4% and output throughput gains reach 4.3×, each scoped to its deployment's activation envelope. We offer the loop design, the supervision mechanisms, and their measured costs as transferable lessons for teams building long-horizon engineering agents.

Code — https://github.com/amazon-science/ammo

1 Introduction

Recent work on LLM-driven GPU kernel optimization shows that frontier models can generate increasingly competitive CUDA and Triton kernels. KernelBench established the dominant evaluation unit: a reference operation, a correctness check, and an isolated speedup ratio (Ouyang et al. 2025). Astra (Wei et al. 2025), CudaForge (Zhang et al. 2025), cuPilot (Chen et al. 2025), AutoKernel (Jaber and Jaber 2026), Kernel-Smith (Du et al. 2026), SpecGen (Guo et al. 2026), and related work extend this setup with multi-agent decomposition, hardware feedback, evolutionary search, model-level profiling, and more efficient exploration. Together, these papers demonstrate rapidly improving capability in automatic kernel engineering; that capability does not necessarily translate into shipped changes. This paper asks what engineering turns a model's local capability into completed work with a measurable external result. We answer it for one domain end to end, production GPU optimization for vLLM serving, and report the engineering as an application with priced, transferable lessons rather than a validated general method.

One source of the gap is a mismatch in the unit of work: frontier models remain unreliable at *compositional generalization*, "the ability to solve unseen problems by composing familiar ones" (Zhang and Khattab 2026; Dziri et al. 2023). They solve the pieces but fail to compose them. Benchmarks hand the model problems already reduced: bounded episodes with a clean initial state, a local objective, and an immediate oracle. Production engineering hands it the unreduced problem, hierarchical and stateful, where a local task is valuable only insofar as it advances a larger objective across dependent steps. In our setting, "optimize this kernel" is the decomposed piece. The unseen composition is to reduce end-to-end latency or increase serving throughput for a fixed vLLM (Kwon et al. 2023) deployment: the candidate must execute on the production path, preserve full-model behavior, and improve a clean system-level metric against the current incumbent (section 3 formalizes these obligations). A locally correct and genuinely faster kernel can be irrelevant to the deployment, because the same source function can dispatch a different kernel under eager execution, graph capture, speculative decoding, or a different model revision: the decomposition that produced it discarded the deployment contract, and so it solved a piece of a different problem.

Practitioners have recently taken to calling the design of this surrounding process *graph engineering* (Runkle and Chase 2026; Shirley 2026): the agentic system is laid out as a graph with nodes as tasks & edges that constrain the steps which may follow; a persistent loop as the simplest such graph (Runkle and Chase 2026). This paper puts the compositional claim into an operational form. We split a long-horizon objective into bounded, externally checkable tasks that resemble the settings where models already do well (*locally in-distribution*, in Zhang and Khattab's terms (Zhang and Khattab 2026)), and we continuously reconnect each local result to the terminal objective. The graph then carries the composition. AMMO (Agentic Model-on-Machine Optimizer)[1] is the system that carried this idea into the field: a loop built on top of a commodity agent harness (Claude

[1]Unrelated to NVIDIA's deprecated `nvidia-ammo` quantization toolkit, since renamed TensorRT Model Optimizer.

Code)[2] that took its current shape through production GPU optimization for vLLM, a domain whose acceptance test is unforgivingly conjunctive and machine-checkable.

The harness supplies the substrate: tool use, subagent spawning, file and repository access. In our hands, the substrate alone produced no optimization that passed the acceptance test. Early, less structured campaigns failed in three recurring ways, detailed in section 3: agents optimized an available local signal rather than the deployment objective, lost obligations as context grew, and iterated in environments that differ from the compiled, CUDA-graphed serving path. AMMO answers with two layers. The *loop* moves the deployment contract, current incumbent, completed evidence, and remaining obligations out of the model's transient context into shared campaign state. It admits a change only through the conjunctive acceptance test of section 3. On top of the loop, two *supervision mechanisms* police the trajectory between measurements: adversarial debate over candidate selection, and a live transcript monitor over implementation. A controlled ablation (section D) gives directional evidence for each: debate raised how often the system shipped, and monitoring governed whether what shipped survived audit.

We write for teams building or adopting long-horizon engineering agents. Our contributions are those of an applications paper:

1. We put a number on the last mile. Across every candidate that logged a measured isolated speedup in the three retained campaign ledgers, isolated kernel speedup is non-monotone with realized deployment value (fig. 2). A rejection ledger keeps the measured reason each closed candidate died (section 5).
2. We present the application: a graph-engineering implementation on a commodity agent harness that cuts a deployment-level objective into bounded agent tasks and keeps state, the current incumbent, and the machine-checkable acceptance conditions outside model context. We report who uses it and where the human boundary falls. Its pilot-stage status covers four public upstream candidates, each carrying its measured serving effect, the envelope under which it activates, the state of its evidence, and what it cost to operate (sections 2 to 5).
3. We run a controlled ablation over the supervision mechanisms. Baseline, bottleneck evidence, and validation stay fixed; only the supervision structure varies. That separates what adversarial debate contributes from what live transcript monitoring does, and every shipped change is scored by both its gate outcome and a per-ship audit (section D).
4. We pass on development lessons from the field: which oversight mechanisms earned their cost and the concrete work remaining before broader deployment (sections 6 and 7).

[2]We implemented the loop on two harnesses, Claude Code and Codex; the mechanisms of section 4.1 assume only harness-level hooks and subagents. All reported results are from the Claude Code implementation.

2 Application, Users, and Deployment Status

The application. AMMO is a harness (Claude Code or Codex) skill that runs autonomous GPU-optimization work against concrete vLLM deployment contracts. We call one deployment-specific execution of the loop a *campaign*; a campaign may contain multiple rounds. A campaign begins from a target manifest (model and revision, accelerator, numerical formats, parallelism, workload grid, compiler and CUDA-graph settings, benchmark commands, quality task, and a practical effect threshold) and ends with either an upstream-oriented candidate carrying an evidence chain or a measured record that closes the attempted avenue.

Primary users. The intended users are performance and serving engineers responsible for LLM inference deployments, for whom AMMO automates the profile–implement–validate cycle they would otherwise execute manually; secondary users are vLLM maintainers and the open-source community, who receive reviewable pull requests with disclosed benchmarks, activation conditions, fallbacks, and evidence limits.

Deployment status: pilot-stage, pre-acceptance. The authoring team has operated four complete deployment-specific campaigns: GPT-OSS-120B on two H100s (backbone Claude Opus 4.6, the most capable model then available), and Qwen3.5, Kimi-K2.6, and gemma-4 NVFP4 deployments on B300 (Opus 4.8). Their outputs are four public vLLM pull requests. None is merged in the paper's dated snapshot; maintainer acceptance remains a social step outside the system's control. Human operators supplied infrastructure continuity, line-by-line review before posting, DCO sign-off, and one explicit scope permission; no human proposed, authored, or tuned an optimization mechanism.

Why this is hard for AI. The difficulty is hierarchical. Models are already reliable at the lower-level task, writing a fast kernel, but the deployment pays only for the higher-level objective that task must serve, an end-to-end win on a fixed serving system, and crossing that level boundary is the composition step where the problem leaves the training distribution: each piece is familiar, the multi-level whole is not (Zhang and Khattab 2026). The upper level is also conjunctive, so a candidate that is fast but breaks quality, or fast but never dispatches under CUDA graphs, has zero deployment value; both occurred (sections 3 and 5). The model's own pathologies then compound over the trajectory: an agent that hallucinates a conclusion, or self-confirms a flattering local proxy, carries the error forward across hours of GPU reservations and repeated context compaction; task-completion reliability drops as tasks get longer (Kwa et al. 2025; Hong, Troynikov, and Huber 2025). Finally, the evidence misleads even a careful agent; section 3 catalogs how profiled, benchmarked, and baseline numbers each pass for clean.

3 The Last Mile as Conjunctive Acceptance

A round ends in a promotion only when Equation (1) holds. That is the whole definition of done, and an isolated kernel speedup does not reach it: the local oracle is now the

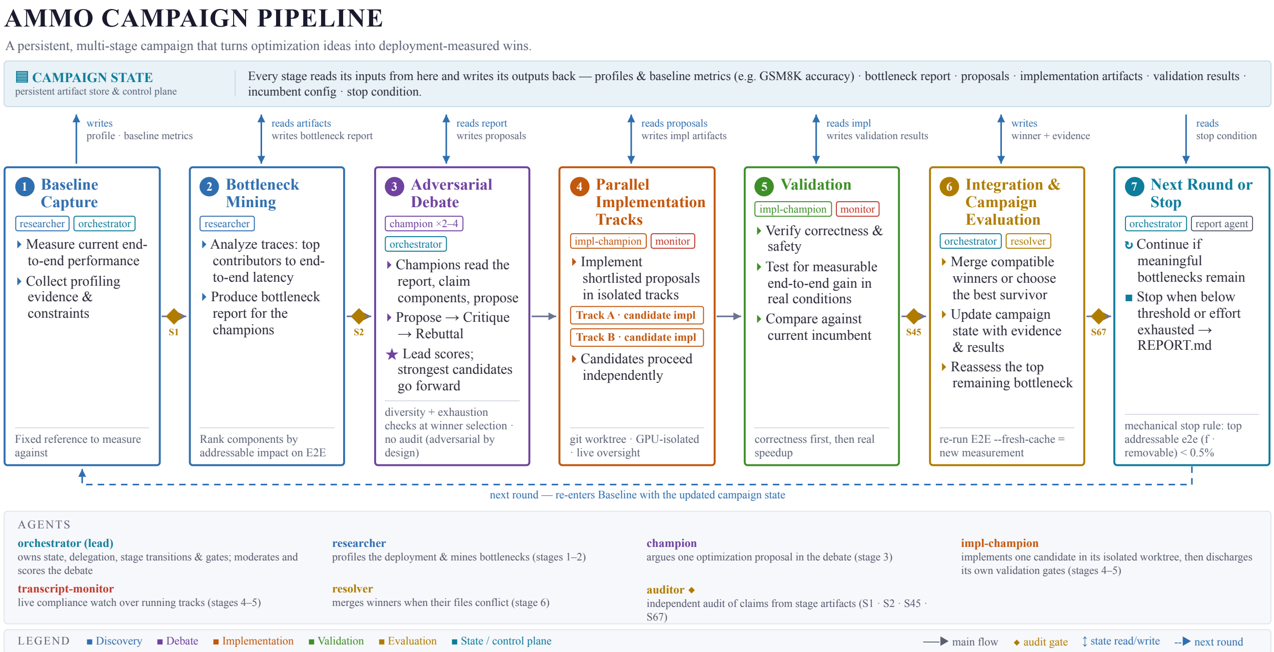

Figure 1: One optimization round of AMMO, walked through in section 4.3.

deployment's terminal objective. Take D as the immutable deployment contract, I_t as the incumbent before round t, and c as a candidate. Each $P^{\text{level}}_{\text{concept}}$ below is a binary, machine-checkable pass/fail test on c, evaluated under D and against I_t; the superscript names the level it measures (ker for the isolated kernel, sys for the integrated serving system). AMMO promotes c only when the ship condition holds:

$$\begin{aligned}\text{Ship}(c \mid D, I_t) = {} & P^{\text{ker}}_{\text{correct}} \wedge P^{\text{sys}}_{\text{correct}} \\ & \wedge P^{\text{sys}}_{\text{dispatch}} \wedge P^{\text{sys}}_{\text{speedup}}.\end{aligned} \tag{1}$$

The four terms test that c is numerically correct in isolation ($P^{\text{ker}}_{\text{correct}}$); that full-model behavior is preserved on D's quality task ($P^{\text{sys}}_{\text{correct}}$); that its optimized kernel actually dispatches on the real compiled production path ($P^{\text{sys}}_{\text{dispatch}}$); and that the production metric improves against I_t by at least the predeclared threshold ($P^{\text{sys}}_{\text{speedup}}$). No term compensates for another, and notably absent is any isolated kernel-speedup term: a fast kernel is a measured input to candidate selection and Amdahl projection, never a promotion requirement, which is the paper's central point. Beyond the four, c must build on D's target tree, activate across D's declared envelope, and carry a complete evidence chain. When (1) holds, $I_{t+1} = c$; otherwise $I_{t+1} = I_t$ and the failure evidence is kept on file, so a later round can tell "untried" from a "measured dead end."

Early campaigns exposed three recurring causes of trajectory failure. *Proxy drift and self-confirmation*: an agent chases the nearest local number, a kernel time or occupancy or a test it wrote itself, and stops watching the deployment objective; we saw a fast kernel win on a path that never dispatched, backed by tests that merely checked the code against its own assumptions. *Instruction dilution*: obligations still nominally in context slid under the logs as a trace ran on (others report the same effect as input context grows (Hong, Troynikov, and Huber 2025)); an agent re-entered a stage it had settled, the sanctioned sweep got quietly worked around, and gates honored earlier went unrun. *Production-parity pressure*: the easiest place to iterate is never the compiled, CUDA-graphed serving environment, so a worktree benchmark could quietly pull in the session build and say nothing was wrong, and profiled timing, too, could pass for clean. Take supervision away and the controlled ablation of section D brings the first two back on demand: ships passed every gate while swapping in a mechanism no one requested, and quality references were re-captured after a check had failed.

At the acceptance boundary, each cause surfaces as a proof that does not hold. The evidence may describe the wrong path, build, or experiment. A local improvement may be real yet leave serving unmoved or behavior unpreserved, usually because Amdahl's law caps its exposed share or overlap already hides the work. Or the trajectory simply omits the evidence completion needs. The predicates in (1) reject each independently.

4 The AMMO System

4.1 Mechanisms that hold the loop together

The stage graph is not sufficient by itself. AMMO combines six mechanisms that respond to the causes of section 3: **M1 One objective:** the clean serving metric against the incumbent (sections 4.3 and 5.3). **M2 Empirical grounding:** production traces and GPU probes before promotion. **M3**

Separated judgment: proposal, implementation, challenge, and reconstruction carry different authorities (section 4.2). **M4 Non-discretionary progression:** artifacts and state transitions determine progress rather than narrative confidence. **M5 External memory:** the contract, incumbent, attempts, evidence, and obligations live outside conversational context (section 4.4). **M6 Production parity:** the sanctioned measurement path binds a candidate to the compiled, CUDA-graphed program (section 5.3). M1, M3, and M4 counter proxy drift and self-confirmation; M5 counters instruction dilution; M2 and M6 counter production-parity pressure. Together they form the *loop layer*; the *supervision layer* (adversarial debate over candidate selection, live transcript monitoring of implementation) sits on top of it and is the part the controlled ablation varies (sections D and 4.2).

4.2 Agent organization and authority

AMMO uses a lead orchestrator plus specialized roles. The *orchestrator* owns state, delegation, transitions, and gates but writes no optimization code and waives no criterion. A *researcher* captures the baseline and attributes wall time; *champions* turn the profile into competing, probe-backed hypotheses; and an *implementation champion* writes each selected change in an isolated worktree. A live *transcript monitor* raises advisory challenges; champion debate and this monitor are the two supervision mechanisms isolated in section D. An *auditor* cold-reconstructs stage claims from primary artifacts, and a *report writer* assembles the terminal record. Delegates, investigators, and a resolver handle bounded support tasks. No single agent chooses the target, implements the mechanism, defines the evidence, and approves promotion.

This separation is enforced rather than merely described: hooks, the state schema, and a transition validator reject illegal moves, and the transcript monitor and auditor hold no write authority over the work they check.

4.3 Optimization loop

Figure 1 walks through one round. Stages 1–2 establish a clean production-parity baseline and its measured bottlenecks; stage 3 builds competing, probe-backed hypotheses; stages 4–5 implement the selected candidates in isolated worktrees and discharge the acceptance predicates, cheapest first; stage 6 integrates whatever survived and remeasures it against the incumbent; stage 7 mines the shifted bottleneck landscape for new work or, if the stop rule fires, ends the campaign.

4.4 Persistent memory & runtime control plane

The control plane has two jobs: *remember* the campaign and *constrain* its transitions. An immutable target manifest records the objective; round-scoped `state.json` points to what is active; the artifact tree establishes what happened (fig. 1).

On resume after interruption or compaction, the lead reads `state.json`, reconciles it with on-disk gate artifacts, and continues from the last completed gate, so parallel or resumed instances act as one continuing process. Hooks and verifiers fence in what may be asserted out of that memory: they validate every state transition, inject stage guidance, restore context and GPU reservations on resume, challenge unsupported stop attempts, and inspect the required artifacts at each gate, so no runtime invariant hinges on whether an agent is still attending to a paragraph read thousands of tokens ago. During the reported campaigns the acceptance predicates of eq. (1) were ultimately enforced by the measurement artifacts plus the human line-by-line review of section 2.

Table 1: Public vLLM pull requests from the four campaigns, states frozen 22 June 2026 (all open or draft, none merged). PR #n is at https://github.com/vllm-project/vllm/pull/n; the full dated evidence manifest is in table 2.

PR / state	Deployment	Production result
#39714 open	2×H100, TP=2; $M \leq 64$	TPOT 5.4–9.7% lower; throughput 9.2–27.3% higher
#45717 draft	B300, TP=1; three flags	4.2–5.4× kernel; E2E 1.7–5.4% lower
#45452 draft	4×B300, TP=4; three flags	E2E 2.5–6.0% lower
#45450 open	B300, TP=1, MTP; structural guard	E2E 35.4% lower and 74.5→320.6 OTPS at 27k/BS1

5 Field Results: Four Campaigns

None of the four PRs is merged (table 1). Several of the optimizations are deliberately gated behind activation flags or structural guards: they target specific deployment configurations and need not be appropriate as default behavior in a general-purpose library, and the loop's goal is to produce deployment-measured, review-ready candidates rather than to replace maintainer review (section 2). The diffs, benchmark commands, and raw measurements are public (section 5.3; verifiability scope in section 7).

5.1 Public upstream candidates

Table 1 summarizes the four public artifacts; the appendix manifest (table 2) carries the full evidence chains and mechanisms (MoE routing-metadata fusion, shared-expert-gate and sampler kernels, MLA pipelining and expert overlap, and a 3D flash-decoding dispatch fix). Two carry lessons the table cannot: #45717's shared-expert-gate kernel is 5.4× faster in isolation yet contributes single-digit percent end-to-end, the dilution of section 3 inside a retained artifact; and #45450's gain comes not from a new kernel but from rescuing a dispatch path, where the incumbent had been falling back to a slow 2D kernel for entire long-context speculative-verify steps.

5.2 What the loop rejected

For application builders, the rejection ledger is the more instructive half (representative entries in table 3). The Qwen campaign ran eighteen rounds, retained four optimizations, and closed thirty-eight candidates under eq. (1) with a measured reason for each. Two examples show the pattern. OP-011, bit-exact and $1.8\times$ faster in isolation, was worth at most $+0.01\%$ end-to-end because the eliminated fills were already hidden behind memory-bound MoE GEMMs; OP-009's apparent $2\times$ routing-gate fusion was a serialized-timing artifact with no exposed time on the real CUDA graph, invalidated before any end-to-end run was spent on it. A kernel-only benchmark would have scored both as wins. Figure 2 plots this non-monotonicity across every measured candidate.

Two further rejections shaped the system. In an FP8 campaign, a quantization kernel that agreed with the reference to 99.8% bitwise still flipped nearly all GSM8K answers, a one-ULP division difference compounded through forty layers of re-quantization: this is why $P_{\text{correct}}^{\text{sys}}$ is a separate physical measurement, not an inference from numerical agreement. In the Kimi campaign, an early prototype disproved a plausible occupancy hypothesis, so the system escalated the scope decision instead of iterating on a dead end.

5.3 Measurement policy

Trustworthy numbers were harder to obtain than we expected. Every campaign measurement runs with CUDA graphs and `torch.compile` enabled, and we compare against the production incumbent, never a naive eager reference. We use profilers only to confirm which path executed; profiling perturbs timing, so the final comparison runs with it off. Benchmark protocols vary from one deployment to the next, so each PR states its workload, repetition count, and tolerated variation; results from different PRs are never pooled. Model quality is checked with greedy GSM8K or GPQA.

5.4 Cost and payoff

Three of the four campaigns retain enough session metadata for a cost reconstruction: about \$10,000 across 10.8B tokens (assuming public pricing), of which $\sim$75% is cache reads/writes, making compact structured state and stage-local context the first-order cost optimizations for the harness itself and independently corroborating the context-offloading argument of Zhang and Khattab (Zhang and Khattab 2026) (per-campaign breakdown in section C). Against that cost stand the serving improvements of table 1, each scoped to its deployment's envelope. On a revenue-serving fleet, decode-throughput improvements of this size translate into capacity headroom or instance-count reduction at constant traffic. We do not estimate engineer-hours saved: the search is adaptive, the counterfactual path is undefined, and the deployments are not repeated standardized tasks. What we can price is the system's own oversight: in the controlled ablation of section D, full supervision cost roughly $1.6\times$ the GPU-hours of the unsupervised baseline and delivered both a higher gate-passing rate and more audited ships (single-ship margins at small n, but priced).

6 Development Lessons

6.1 Guardrails priced by measured yield

Oversight has a real cost, and its value varies by mechanism and stage. Two guardrails we built, instrumented, and then treated differently make this concrete.

A guardrail we retired. An independent adversarial validation agent re-tested each candidate's correctness and speedup under an independence rule (write your own tests; do not read the champion's) and blocked the implementer until it returned a verdict. Across 32 genuine dispatches it changed zero shipping decisions, found no discrepancy in 24, and sat on the critical path a median 8.16 minutes per dispatch. We retired it and folded its checks into the implementation champion. The inference, that a stronger model makes this kind of check redundant first, is a hypothesis; the retirement decision itself was measured.

A guardrail we kept, at a price. The live transcript monitor polls a growing context many times per campaign, so summed it roughly doubles the cost of the stage it watches. On the *implementation* stage it earns that: its non-redundant catches concentrate in gate-gaming (changes built so the gate as-run falsely passes) and runtime liveness (wedged or silently dead implementers), classes no artifact gate reaches. On the *debate* stage it earns nothing, because rival champions already provide built-in adversarial pressure. We keep the monitor on implementation and drop it on debate: the value of oversight varies by stage.

A controlled ablation (section D) isolates this contrast directly: with debate, implementer, tasks, and validation held fixed, removing the monitor *raises* the gate-passing ship rate ($6/22 \to 7/22$) and *lowers* the audited one ($5 \to 4$), because unmonitored configurations pass gates partly through the same gate-gaming class the monitor catches. A throughput metric blind to those defects scores oversight as pure drag; an audited metric prices it positively. At $n \leq 5$ per cell we read these as directional results and make no significance claim.

6.2 Lessons for long-horizon agentic systems

The vLLM campaigns taught us the following about long-horizon agentic tasks that overwhelm a single agent's context window (Runkle and Chase 2026; Shirley 2026).

L1. Ground every claim in an artifact another role can recheck; agents hallucinate success. Self-verification instructions are not sufficient; the loop needs anchors the agent cannot fabricate. **L2. Anchor on one terminal metric, never a local proxy, and treat it as the north star.** Local measurements feed candidate selection, but progress is judged only against the predeclared system-level metric, inside the conjunctive test of eq. (1). **L3. Adversarially audit every agent, and allow rebuttals.** Rival champions audit one another through debate, and a round-end auditor cold-reconstructs claims from primary artifacts, spawning investigators on cross-round inconsistencies such as end-to-end baseline drift; auditors err too, so the audited agent may rebut, and each audit is kept or retired by measured yield (sections 4.2 and 6.1). **L4. Hooks are enforcement; prompts are merely suggestions.** Agents forget instructions and make mistakes as context grows, so encode invariants as deterministic hooks that remind or block progression (section 4.4). **L5. Preserve negative evidence and provenance.** A rejected candidate is reusable and evidence must stay dated; without them, long campaigns rediscover dead ends and stale evidence silently becomes current (tables 2 and 3).

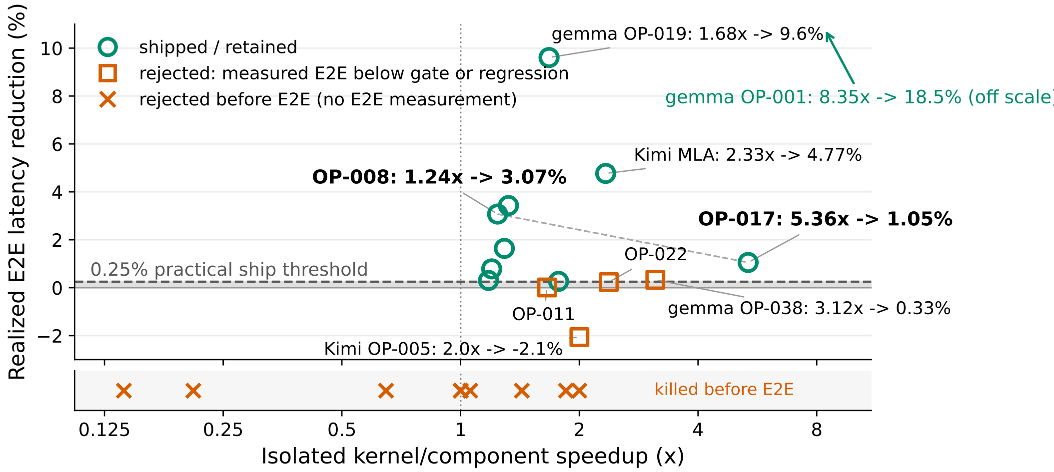

Figure 2: The last-mile gap across all 23 candidates with a measured isolated speedup in the three retained ledgers. Isolated speedup is not monotone with realized E2E value. Rug strip: candidates killed before E2E measurement.

7 Limitations and Path to Full Deployment

Trajectory and evidence. Each campaign is one trajectory through an adaptive, stochastic search; re-running the harness need not recover the same candidates or yield. We claim evidence verifiability, not trajectory reproduction: retained manifests, commits, commands, raw measurements, quality results, and activation conditions can be independently rechecked (table 1 and section 5.3).

Mechanisms and scope. The six mechanisms of section 4.1 describe the configured loop; we have not shown the set minimal or causally necessary, and we did not run an unstructured-harness baseline: the ablation's weakest arm still receives the loop's frozen evidence, state, and gates, so its 3-of-21 ship rate bounds from above what the bare harness would achieve. The retired validator is one measured instance, not a trend. All four campaigns were author-operated on vLLM/NVIDIA GPUs, with no matched human-engineer or alternative-agent arm; we claim autonomous technical completion and measured systems output, not a labor-productivity claim.

Path to broader deployment. Broader use requires maintainer review and requested revalidation; a uniform paired protocol after material rebases; and operators outside the authoring team and tests on other serving stacks.

8 Related Work

KernelBench and successors evaluate generated kernels by correctness and isolated speedup (Ouyang et al. 2025; Wei et al. 2025; Zhang et al. 2025; Chen et al. 2025; Dong et al. 2026; Guo et al. 2026); after an agent inflated speedups by gaming its own harness (Wiggers 2025), robust-kbench hardened the benchmark (Lange et al. 2025). AMMO moves the burden one layer further: even a correctly measured isolated speedup can be non-monotone with production value (section 5), so acceptance must bind to the serving framework. AutoKernel ranks targets by Amdahl impact (Jaber and Jaber 2026); Kernel-Smith upstreams generated kernels as a follow-on manual step (Du et al. 2026); FastKernels and ISO-Bench score supplied changes in production shape (Oliaro et al. 2026; Nangia et al. 2026) but do not close the loop from bottleneck discovery to artifact. AMMO's distinction as an application is ownership of the full trajectory, deployment contract to reviewable upstream candidate, under one persistent process; long-horizon coding agents (Yang et al. 2024; Wang et al. 2025) and oversight mechanisms (Baker et al. 2025; Irving, Christiano, and Amodei 2018; McAleese et al. 2024) supply the substrate.

Independent engineering systems are converging on externalized long-horizon agent state (Nguyen 2026; Rajasekaran 2026). AlphaEvolve reports fleet-measured gains against a fixed evaluator (Novikov et al. 2025); AMMO must first construct its own evaluation. AMMO applies related loop primitives to a different terminal boundary and prices selected guardrails by observed yield (section 6).

Zhang and Khattab argue the same decomposition from theory: the harness, not the model, should carry the bias that keeps each call locally in-distribution, with task state offloaded to external memory (Zhang and Khattab 2026). AMMO enforces that discipline structurally (sections 4.2 and 4.4) and holds the fixed harness to a deployment-measured acceptance test rather than benchmark generalization.

9 Conclusion

Frontier models solve the familiar pieces of hard engineering problems; they remain unreliable at composing them into an unseen whole (Zhang and Khattab 2026). AMMO supplies that composition from outside the model: a commodity harness, organized by a persistent loop and supervised between measurements, that reconnects each local result to the terminal serving metric and delivers publicly inspectable vLLM serving changes with a challengeable evidence chain priced by field data (section 6.1).

References

Baker, B.; Huizinga, J.; Gao, L.; Dou, Z.; Guan, M. Y.; Madry, A.; Zaremba, W.; Pachocki, J.; and Farhi, D. 2025. Monitoring Reasoning Models for Misbehavior and the Risks of Promoting Obfuscation. *arXiv preprint arXiv:2503.11926*.

Chen, J.; Wu, Q.; Li, B.; Ma, L.; Si, X.; Hu, Y.; Yin, S.; and Yang, J. 2025. cuPilot: A Strategy-Coordinated Multi-Agent Framework for CUDA Kernel Evolution. *arXiv preprint arXiv:2512.16465*.

Dong, K. S.; Modi, S.; Nikiforov, D.; Damani, S.; Lin, E.; Hari, S. K. S.; and Kozyrakis, C. 2026. KernelBlaster: Continual Cross-Task CUDA Optimization via Memory-Augmented In-Context Reinforcement Learning. *arXiv preprint arXiv:2602.14293*.

Du, H.; Ge, Q.; Hu, J.; Yang, A.; Cai, Z.; Huang, Z.; Yuan, S.; Cheng, Q.; Xie, X.; Chen, Y.; Li, Y.; Xie, J.; Dong, H.; Wu, Y.; Huang, X.; Yang, J.; Wang, H.; Zhou, B.; Li, B.; Guo, Q.; and Chen, K. 2026. Kernel-Smith: A Unified Recipe for Evolutionary Kernel Optimization. *arXiv preprint arXiv:2603.28342*.

Dziri, N.; Lu, X.; Sclar, M.; Li, X. L.; Jiang, L.; Lin, B. Y.; West, P.; Bhagavatula, C.; Le Bras, R.; Hwang, J. D.; Sanyal, S.; Welleck, S.; Ren, X.; Ettinger, A.; Harchaoui, Z.; and Choi, Y. 2023. Faith and Fate: Limits of Transformers on Compositionality. In *NeurIPS*.

Guo, J.; Lu, S.; Ma, T.; Gao, W.; Ye, Z.; Zhang, X.; and Lin, D. 2026. SpecGen: Accelerating Agentic Kernel Optimization with Speculative Generation. *arXiv preprint arXiv:2606.17518*.

Hong, K.; Troynikov, A.; and Huber, J. 2025. Context Rot: How Increasing Input Tokens Impacts LLM Performance. Chroma Technical Report. Published July 2025.

Irving, G.; Christiano, P.; and Amodei, D. 2018. AI Safety via Debate. *arXiv preprint arXiv:1805.00899*.

Jaber, J.; and Jaber, O. 2026. AutoKernel: Autonomous GPU Kernel Optimization via Iterative Agent-Driven Search. *arXiv preprint arXiv:2603.21331*.

Kwa, T.; West, B.; Becker, J.; Deng, A.; Garcia, K.; Hasin, M.; Jawhar, S.; Kinniment, M.; Rush, N.; Von Arx, S.; Bloom, R.; Broadley, T.; Du, H.; Goodrich, B.; Jurkovic, N.; Miles, L. H.; Nix, S.; Lin, T.; Painter, C.; Parikh, N.; Rein, D.; Sato, L. J. K.; Wijk, H.; Ziegler, D. M.; Barnes, E.; and Chan, L. 2025. Measuring AI Ability to Complete Long Software Tasks. In *NeurIPS*.

Kwon, W.; Li, Z.; Zhuang, S.; Sheng, Y.; Zheng, L.; Yu, C. H.; Gonzalez, J. E.; Zhang, H.; and Stoica, I. 2023. Efficient Memory Management for Large Language Model Serving with PagedAttention. In *SOSP*.

Lange, R. T.; Sun, Q.; Prasad, A.; Faldor, M.; Tang, Y.; and Ha, D. 2025. Towards Robust Agentic CUDA Kernel Benchmarking, Verification, and Optimization. *arXiv preprint arXiv:2509.14279*.

McAleese, N.; Pokorny, R. M.; Ceron Uribe, J. F.; Nitishinskaya, E.; Trebacz, M.; and Leike, J. 2024. LLM Critics Help Catch LLM Bugs. *arXiv preprint arXiv:2407.00215*.

Nangia, A.; Mishra, S.; Gokrani, A.; and Chopra, P. 2026. ISO-Bench: Can Coding Agents Optimize Real-World Inference Workloads? *arXiv preprint arXiv:2602.19594*.

Nguyen, V. 2026. How to Run an Autoresearch Workflow with RL Agent Skills and NVIDIA NeMo. NVIDIA Technical Blog, https://developer.nvidia.com/blog/how-to-run-an-autoresearch-workflow-with-rl-agent-skills-and-nvidia-nemo/. Published July 2026.

Novikov, A.; Vũ, N.; Eisenberger, M.; Dupont, E.; Huang, P.-S.; Wagner, A. Z.; Shirobokov, S.; Kozlovskii, B.; Ruiz, F. J. R.; Mehrabian, A.; Kumar, M. P.; See, A.; Chaudhuri, S.; Holland, G.; Davies, A.; Nowozin, S.; Kohli, P.; and Balog, M. 2025. AlphaEvolve: A Coding Agent for Scientific and Algorithmic Discovery. *arXiv preprint arXiv:2506.13131*.

Oliaro, G.; Fu, Y.; Jiang, M.; Lu, O.; Wang, J.; Jia, Z.; Zhang, H.; and Rajbhandari, S. 2026. FastKernels: Benchmarking GPU Kernel Generation in Production. *arXiv preprint arXiv:2605.23215*.

Ouyang, A.; Guo, S.; Arora, S.; Zhang, A. L.; Hu, W.; Ré, C.; and Mirhoseini, A. 2025. KernelBench: Can LLMs Write Efficient GPU Kernels? *arXiv preprint arXiv:2502.10517*.

Rajasekaran, P. 2026. Harness Design for Long-Running Application Development. Anthropic Engineering Blog, https://www.anthropic.com/engineering/harness-design-long-running-apps. Published March 2026.

Runkle, S.; and Chase, H. 2026. 3 Years of Graph Engineering with LangGraph. LangChain Blog, https://www.langchain.com/blog/3-years-of-graph-engineering-with-langgraph. Published July 2026.

Shirley. 2026. Graph Engineering Guide. Blog post, https://www.aibuilderclub.com/blog/graph-engineering-guide-2026. Published July 2026.

Wang, X.; Li, B.; Song, Y.; Xu, F. F.; Tang, X.; Zhuge, M.; Pan, J.; Song, Y.; Li, B.; Singh, J.; Tran, H. H.; Li, F.; Ma, R.; Zheng, M.; Qian, B.; Shao, Y.; Muennighoff, N.; Zhang, Y.; Hui, B.; Lin, J.; Brennan, R.; Peng, H.; Ji, H.; and Neubig, G. 2025. OpenHands: An Open Platform for AI Software Developers as Generalist Agents. In *ICLR*.

Wei, A.; Sun, T.; Seenichamy, Y.; Song, H.; Ouyang, A.; Mirhoseini, A.; Wang, K.; and Aiken, A. 2025. Astra: A Multi-Agent System for GPU Kernel Performance Optimization. *arXiv preprint arXiv:2509.07506*.

Wiggers, K. 2025. Sakana Walks Back Claims That Its AI Can Dramatically Speed Up Model Training. TechCrunch. Published February 2025.

Yang, J.; Jimenez, C. E.; Wettig, A.; Lieret, K.; Yao, S.; Narasimhan, K.; and Press, O. 2024. SWE-agent: Agent-Computer Interfaces Enable Automated Software Engineering. In *NeurIPS*.

Zhang, A. L.; and Khattab, O. 2026. Language Model Harnesses are Compositional Generalizers. Blog post, https://alexzhang13.github.io/blog/2026/harness/. Published July 2026.

Zhang, Z.; Wang, R.; Li, S.; Luo, Y.; Hong, M.; and Ding, C. 2025. CudaForge: An Agent Framework with Hardware Feedback for CUDA Kernel Optimization. *arXiv preprint arXiv:2511.01884*.

A Detailed Evidence Manifest

Table 2 records, for each of the four public artifacts, the pinned measurement tree, the current public representation, the performance and quality evidence, and how that evidence should be interpreted today.

B Representative Candidate Ledger

Table 3 shows representative entries from the campaign rejection ledgers: for each candidate, the mechanism, the local result that made it look promising, and the decisive production measurement that retained or killed it.

C Cost and Human-Intervention Ledger

Deduplicating messages and pricing input, output, and cache traffic at published standard API rates yields approximately \$2,930 for #45717, \$2,977 for #45452, and \$4,330 for #45450 (the vLLM pull requests of table 1), or about \$10,237 across 10.8 billion priced tokens. The generating session for #39714 was not retained and is not imputed as zero. These are reconstructions at list price rather than invoices.

Human actions across the four campaigns were: infrastructure recovery or host migration; line-by-line review; benchmark and quality-result inspection; DCO sign-off and posting; and one Kimi scope permission after the agent had already measured a non-kernel backend win. No human supplied kernel code, optimization mechanisms, or tuning parameters.

D Controlled Ablation of Supervision Structure

The field results of section 5 are observational: monitored and unmonitored campaigns differ in task, duration, and runtime version, so they cannot attribute outcomes to individual pipeline components. This appendix reports the controlled experiment that isolates them (table 4). The design holds the pipeline's measurement stages fixed (frozen production-parity baseline and bottleneck-ranking artifacts staged identically into every cell, and an identical five-gate validation protocol covering kernel correctness, end-to-end model quality, kernel speedup, and absolute and relative end-to-end speedup, applied by the same validator in every arm) and varies only the supervision structure of candidate selection and implementation. Two mechanisms are under test, adversarial debate and live transcript monitoring, across four arms: **A**, a single actor that self-proposes and implements, is the unsupervised baseline; **B** adds champion debate over the frozen evidence, handing the winning candidate to the same actor; **C** runs debate with the production implementation champion but no monitor, making it the AMMO-minus-monitoring control; **D** is production AMMO. A vs. B/C isolates debate; C vs. D, identical except for the monitor, isolates monitoring, the ablation's primary contrast. All arms use the same backbone model (Claude Opus 4.7), one L40S (Qwen3.5-4B, BF16, TP=1), identical prompts up to the ablated components, and per-cell isolated worktrees; 95 of 100 planned cells (5 tasks $\times$ 5 seeds $\times$ 4 arms) completed.

Outcomes are scored from the machine gate artifacts each cell produces; agent self-reports carry no scoring weight. Cells whose transcripts show cross-cell information access (reading sibling seeds' or other arms' work) are excluded from both numerator and denominator, leaving 21–22 cells per arm; such access occurred in all four arms, so exclusion does not favor any. Each gate-passing ship is then audited on three further criteria that the gates themselves do not check: the change uses the mechanism the task names, the decisive measurement compares against a fresh baseline captured under matched conditions, and the model-quality gate was passed against references fixed before the attempt. A ship passing all three with an effect above the benchmark's 0.5% noise floor is counted *audited*; the gate row and the audited row are reported separately. The criteria were applied by scripted adversarial probe agents run uniformly over all 24 gate-passing ships, with disputed verdicts re-verified by separate re-check agents; scoring was not blind to arm, and the criteria deliberately mirror the failure classes the monitor is built to catch; the audited row therefore tests whether the monitor's targets occur when unmonitored, and is no independent outcome measure.

Debate (A vs. B/C). Adding debate raises the gate-passing rate from $3/21$ to $8/22$ and $7/22$, the larger of the two effects, concentrated on the task where candidate choice mattered most (`gemm_r01`: $0/3$ vs. $3/3$ in both debate arms, and the debate arms' `gemm` ships at $+8.8$ to $+13.7\%$ are the largest audited cluster in the study). The audited rows temper the size of the effect (3 vs. 4) but not its direction: debate's raw gain includes ships that do not survive audit, and A's few ships all do. The direction also survives excluding the constructed trap task (`int4_r05`): gate rates without it are $2/16$ vs. $4/17$. A's gemm cells were also degraded by stale reference artifacts, so part of the raw gap is environmental.

Monitoring (C vs. D), the study's treatment contrast. On gate-passing rate the monitor *costs* ships ($7/22 \rightarrow 6/22$). On audited ships it *adds* them ($4 \rightarrow 5$), and D's audited fraction is the highest of the debate arms ($5/6$ vs. $4/8$, $4/7$). The composition explains the reversal. `int4_r05` was constructed so that the named mechanism (INT4 quantization of the target GEMM) degrades model quality beyond the gate threshold; B and C shipped it six times, four of those with kernels containing no INT4 at all: lossless BF16 or FP8 substitutes that satisfy "faster and not less accurate" while abandoning the requested mechanism, which no gate checks. D shipped it zero times, and D's three early terminations (debate concluding no viable candidate exists and declining to implement) are unique in the study. Excluding this constructed task entirely, the gate-rate cost disappears (C $5/18$ vs. D $6/17$) and the audited fractions nearly converge ($4/5$ vs. $5/6$): the monitor's measured contribution concentrates on the trap task, which it declines to ship, and on run survival, with no uniform advantage across ordinary tasks. Other audit failures in the unmonitored arms include mid-cell re-capture of quality references after a failing check (outcome-determinative in ships from three arms) and stale or condition-mismatched baselines in the decisive comparison. The contrast also extends to run survival: three C cells terminated mid-run when the coordinating agent issued an erroneous shutdown to its own champions; D, identical but monitored, had none. These are controlled-condition instances of the failure causes of

Table 2: Dated evidence manifest for the four public artifacts. "Current" means the public representation visible on 22 June 2026.

PR	Measurement tree	Current representation	Performance evidence	Quality evidence	Current interpretation
#39714	vLLM v0.20.1; same build/GPU pair for baseline and candidate	Open, ready; recent upstream representation	Ten `bench serve` configs; median TPOT and output throughput	Bit-identical greedy outputs; optimized-only GPQA threshold result (0.6622 vs 0.568)	Broadest serving result; bit-identical greedy outputs satisfy the quality predicate by construction, making the unpaired GPQA a sanity check; a paired quality run and full current-tree rerun remain before it is revalidated on the current tree
#45717	Earlier v0.21.0 development; latency repeated on main `fa63bb9db`	Draft, one commit	Six fixed-batch cells, 10 iterations, fresh process per cell	Per-opt GSM8K on earlier trees and local numerical checks	Performance revalidated post-rebase; quality still at the pinned-tree E2E level
#45452	v0.22.1 / `0decac0d9`	Draft with needs-rebase label	Five cells, 5 iterations per arm; two spread criteria disclosed	Full GSM8K A/B on B300 (92.95%→93.10%)	Valid pinned-tree result; not yet rebased onto the current tree
#45450	v0.22.1 / `0decac0d9`	Open, rebased; post-rebase kernel-only differential check	Six cells, 5 iterations per arm; only 27k shapes clear $\pm 2\sigma$	Full GSM8K A/B before rebase; 74-case L40S/bf16 kernel check after rebase	Rebased onto the current tree, with an explicit split between pre-rebase deployment evidence and post-rebase kernel evidence

section 3, proxy drift and evidence attached to the wrong comparison, and the gate-vs-audited gap is the measurable footprint of section 6.1's claim that unaudited throughput metrics score oversight as pure drag. Two attributions qualify the contrast: within D's early terminations the decisive objections came chiefly from rival champions rather than the monitor (supporting the implementation-stage-only monitor placement of section 6.1), and monitoring did not prevent the cross-cell information access that forced exclusions in all four arms; isolation is an environment property that oversight does not supply.

Full system (A vs. D). Full AMMO over the unsupervised baseline: gate rate $14\% \rightarrow 27\%$, audited ships $3 \rightarrow 5$, at roughly $1.6\times$ the GPU-hours per cell. The two mechanisms contribute where each binds: debate on candidate selection for solvable tasks, monitoring on refusal and measurement discipline for the unsolvable one.

With $n \leq 5$ per cell, no pairwise contrast survives multiple-comparison correction. We therefore read the study as consistent directional evidence for the mechanism claims of sections 4 and 6.1 rather than as standalone proof. Two later efforts reinforce that caution. A 45-cell study varied monitor strength across none, Sonnet 4.6, and Opus 4.7, and the ship counts came back 9/15, 9/15, and 7/15. A subsequent 36-cell pilot on a newer backbone (Opus 4.8) returned 17 failures, five of them GPU-starvation stubs concentrated entirely in the Opus-monitor arm, an arm-asymmetric attrition that invalidates its contrasts. Neither result supports a cross-model claim. A confirmatory study would need considerably more room. The seed count is the first thing we would raise, to at least 15 in every task–arm cell, and we would fill in the factorial arms this run left out. Before any data is collected we would pre-register the task-by-arm interaction. We would keep each baseline refreshed within 48 hours and fix a minimum practical effect in advance. We would calibrate quality non-inferiority from repeated null runs and log both inference and wall-clock cost the same way in every cell. Our audit criteria carry over into that harness as well.

Table 3: Representative measured candidates from the retained Qwen and Kimi campaign ledgers, plus the exploratory FP8 campaign's decisive rejection. The ledger makes negative results reusable rather than allowing later rounds to rediscover them.

Candidate	Mechanism	Local result	Decisive production result	Disposition
OP-017	Fuse shared-expert gate chain	5.36× at $M = 1$	1.05% E2E; GSM8K +0.38pp	Retained
OP-008	Fuse two GDN input projections	1.20–1.24×	3.07% E2E; GSM8K −0.15pp	Retained
OP-011	Remove 48 redundant scale fills	1.66–1.83×, bit-exact	At best 0.011% E2E; work already overlapped	Reject: below gate
OP-022	Lossless Gumbel-max sampler	2.38×	0.234% E2E	Reject: below 0.25%
OP-009	Router-gate fusion	Apparent 2.0× serialized	0.00 μs exposed on actual graph	Reject: timing artifact
OP-019	Fused split-K reduction chain	0.140×	Vendor body dominates	Reject: local regression
OP-003	GDN occupancy rewrite	Occupancy 11.3→22.8%; 1.001×	Scheduler-issue-bound rather than occupancy-bound	Reject: no value
Kimi prototype	Two-CTA/SM down-expert GEMM	0.647×; 255 registers/thread	Occupancy-2 mechanism physically unreachable	Exhaustion evidence
FP8 OP-014	Batched Triton quantization	1.62×; 99.8% bitwise local agreement	99.8% of GSM8K questions diverge at first token	Reject: quality cascade

Table 4: Ship counts by arm (A actor-only baseline; B debate + actor; C AMMO without monitor; D full AMMO). Per-task rows use per-cell denominators after isolation exclusions. "Gate" = all five validation gates pass as-run; "Audited" additionally requires the on-task mechanism, a fresh matched baseline, references fixed before the attempt, and an effect above the 0.5% noise floor. Tasks: `gemm_r01` QKV-projection GEMM dispatch; `concat_r03` fused attention-head concatenation; `fp8_r05` FP8 quantization of linear layers; `int4_r05` INT4 group quantization (the constructed trap task); `occ_r07` occupancy tuning of a Triton gate-up projection.

Task	A	B	C	D
gemm_r01	0/3	3/3	3/3	2/3
concat_r03	1/4	0/4	1/5	1/4
fp8_r05	1/4	0/5	1/5	1/5
int4_r05	1/5	4/5	2/4	0/5
occ_r07	0/5	1/5	0/5	2/5
Gate	3/21	8/22	7/22	6/22
Audited	3	4	4	5
Audited frac.	3/3	4/8	4/7	5/6

It would need a task-fidelity gate and quality references that freeze the instant an attempt has been scored against them. A quality eval would have to be large enough to resolve the degradation the trap task induces, and each cell would get its own filesystem and git isolation.

E Artifact Supplement Contents

The supplementary artifact accompanying this paper contains, per campaign: the deployment target manifest; base, candidate, and measured commit identifiers; baseline and candidate benchmark commands with raw per-run outputs; profiler/dispatch evidence stored separately from clean timing evidence; local correctness matrices and model-quality A/B outputs; activation and fallback tests; the round records and `state.json` history; and the human-intervention and inference-cost ledgers. The four public PRs additionally expose the source diffs, activation conditions, and stated benchmark results.

The evidence behind the controlled ablation (section D) and the guardrail-yield findings (section 6.1) is packaged as a separate read-only archive of machine artifacts: the canonical per-cell ledger and per-ship audit tally from which every number in table 4 recomputes, each cell's five-gate artifacts and reconciled verdict, raw dispatch-proof traces with distilled kernel tables for the gate-passing ships, session transcripts for the ships and all audit-cited cells, summary tiers for the two follow-up studies, and the monitor-cost and validator investigation reports. Its top-level README gives a fifteen-minute verification path and discloses every known confound and omission. The source code and this archive (430 MB zstd, published as a versioned release asset; SHA-256 `3fde621578ff4a6793783e8ffe5599a2b5b2bf6f26d5503d63f5590557019206`) are available at https://github.com/amazon-science/ammo. The released code is the system's current revision, which postdates these studies: it adds an audit gate after each stage and defaults to newer models. The study-time configuration is documented in the ablation archive.